CXCL5 Promotes the Malignant Phenotype of Pancreatic Cancer and Is Associated With Immune Infiltration

Tao Wang[1,2]* (ID), Jian Sheng[3]*, Xiaoguang Wang[2], Minyuan Zhu[2], Shijun Li[1], Yiyu Shen[2] and Bin Wu[2]

[1]Graduate School, Zhejiang Chinese Medical University, Hangzhou, China. [2]Department of Hepatobiliary Surgery, The Second Affiliated Hospital of Jiaxing University, Jiaxing, China. [3]Department of Science and Education, The Second Affiliated Hospital of Jiaxing University, Jiaxing, China.

ABSTRACT

BACKGROUND: The significance of CXCL5 in pancreatic cancer is unclear, although it has been implicated in the malignant process of many different types of cancer. Research on the impact of CXCL5 on immune cell infiltration and the malignant phenotype of pancreatic cancer is needed. This study aimed to examine the connection between CXCL5 expression and immune cell infiltration and the malignant phenotype of pancreatic cancer.

METHODS: Tissue samples and clinical information were collected from 90 patients with pancreatic cancer. Tumour tissues and adjacent tissues were made into a tissue microarray and stained for immunohistochemistry analysis. Reverse transcription-quantitative polymerase chain reaction (RT-qPCR) and Western blot analysis were performed to measure the expression level of CXCL5. CXCL5-overexpressing/CXCL5-knockdown cell lines were constructed via transfection for cytological experiments. CCK-8, cell apoptosis, cell cycle, cell invasion, and cell colony formation assays were used to detect the effect of CXCL5 on the malignant phenotype of pancreatic cancer cells. Finally, a mouse model of pancreatic cancer was constructed for in vivo verification.

RESULTS: Compared with control cells, pancreatic cancer cells overexpressing CXCL5 exhibited increased proliferation, migration, and invasion but decreased apoptosis. Conversely, knockdown of CXCL5 did not enhance the malignant phenotype of pancreatic cancer cells. Spearman correlation analysis indicated that there was a significant negative correlation between CXCL5 levels and the CD8 IRS. However, there was a significant positive correlation between FOXP3 IRS and CXCL5 levels.

CONCLUSIONS: CXCL5 is highly expressed in pancreatic cancer and promotes the malignant phenotype of pancreatic cancer cells. CXCL5 is associated with immunosuppressive FOXP3 + T-cell infiltration, which facilitates the formation of an immunosuppressive microenvironment (with low CD8 + T-cell infiltration).

KEYWORDS: CXCL5, pancreatic cancer, malignant phenotype, immune infiltration, tumour microenvironment

Introduction

Pancreatic cancer is an aggressive tumour with a poor prognosis and a high mortality rate. Among cases, 90% of pancreatic cancers are of the pancreatic ductal adenocarcinoma (PDAC) pathological type, and its 5-year survival rate is only 9%.[1,2] However, the prognosis of patients can be improved by surgical resection of tumours. However, because the early signs of pancreatic cancer are not obvious, many patients present with late-stage disease at diagnosis, so they miss the opportunity for surgery.[3] Accordingly, better treatment options are needed for patients with unresectable pancreatic cancer as well as patients who have undergone surgery.

At present, the carcinogenic mechanism of pancreatic cancer is still unclear, and the current clinical treatment is mainly based on moderately hypofractionated chemoradiotherapy.

Targeted immunotherapy and neoadjuvant therapy have also achieved a certain degree of clinical efficacy. However, the survival time of most patients is not significantly prolonged.[3-5] We first assessed the tumour microenvironment to further explore treatment regimens for improving patient survival. During the growth of pancreatic cancer, the interaction of cells from the tumour microenvironment plays a pivotal role. The cells and soluble factors in the microenvironment may provide more effective targets for pancreatic tumour treatment.[6] The tumour microenvironment of pancreatic cancer has special characteristics. It mainly includes connective tissue hyperplasia and immune cells. These properties support the low immunogenicity of these tumours.[7,8] The tumour microenvironment also affects tumour growth. One study pointed out that senescent cells can enhance tumour paracrine function.[9] There may also be a correlation between tumour immune escape and immune

---

* Tao Wang and Jian Sheng contributed equally to this work.

cell infiltration, such as CD4 + and CD8 + T lymphocyte infiltration, which is significantly decreased in pancreatic cancer tissues compared with control tissues. Therefore, enhancing such immune infiltration may become an effective treatment strategy.[10,11] CXCL5 is present in the tumour microenvironment. During the apoptotic death of tumour cells, CXCL5 is released into the microenvironment. CXCL5 overexpression improves the invasive capacity of tumour cells and reduces immune invasion.[12,13] As a member of the CXC chemokine family, CXCL5 suppresses immune cell infiltration through specific binding to the G protein-coupled receptor CXCR2.[14] CXCL5 promotes malignant phenotypes in various cancers and participates in tumour progression through autocrine and paracrine pathways in prostate cancer,[15] osteosarcoma,[16] and hepatoblastoma.[17] A meta-analysis comprehensively analysed a variety of tumours, and high CXCL5 in tumours was found to predict a worse prognosis.[18]

Whether CXCL5, which is overexpressed in pancreatic tumours, further affects the infiltration of various immune-related cells into tumour tissues and whether it has an impact on the survival of patients with advanced pancreatic tumours are unclear. These connections deserve our study.

Materials and Methods

Patients and tissue samples

For this study, the clinical data of 90 patients with pancreatic cancer were collected from the Second Affiliated Hospital of Jiaxing University between 2012 and 2021. All patients underwent surgery, and the postoperative pathology clearly confirmed pancreatic cancer. The clinical data included age, sex, tumour site, tumour size, TNM stage (eighth edition of the guidelines of the American Joint Commission on Cancer, 8th AJCC), and the statuses of local invasion, perineural invasion, vascular invasion, lymph node metastasis, smoking, drinking, and diabetes. Exclusion criteria were as follows: (1) received any anti-tumour treatment before surgery; (2) the tumour was confirmed as non-pancreatic cancer by postoperative pathology; (3) merge with other malignant tumours; and (4) the enrolled cases do not have complete clinical information data. The relationships between the expression of CXCL5 in these patients and these clinical variables were analysed.

Immunohistochemistry and interpretation

The Tissue microarray (TMA) paraffin sections (4μm) were dewaxed in xylene and gradient ethanol solutions. The specimens were stained with an anti-CD8 antibody after citrate antigen retrieval (Maixin, MAB-0021, 1:4000), an anti-CD4 antibody (Maixin, RMA-0021, 1:30000), an anti-FOXP3 antibody (Abcam, ab20034, 1:50), and an anti-CXCL5 antibody (R&D, MAB254, 1:50). We eliminated image spots originating from the preparation or staining operations. Subsequently, using microscopic observation, 2 independent pathologists analysed these TMA readings (blinded to each patient's clinical data). These

digital images were passed through the Aperio ImageScope digital pathology system for data analysis. The immunoreactivity score (IRS) method was used for immunological scoring. IRS was calculated as follows: immunohistochemical staining intensity score × score for the percentage of positive cells. In general, the overall staining intensity was scored from 0 to 3, with 0 = no staining, 1 = weak staining, 2 = moderate staining, and 3 = strong staining. The percentage of positive cells was scored from 0 to 4, with 0 = 0% stained cells, 1 = 1% to 10% stained cells, 2 = 11% to 50% stained cells, 3 = 51% to 80% stained cells (strong reaction), and 4 = 81% to 100% stained cells. Therefore, the final IRS ranged from 0 to 12.

Cell culture

Human pancreatic adenocarcinoma cells (BxPC-3, CFPAC-1, ASPC-1, Panc-1, and SW1990) and human normal pancreatic ductal epithelial cells (HPDE6C7) were acquired from Shanghai Qingqi Biotech Co, Ltd. All cell lines were cultured in Iscove's modified Dulbecco medium (IMDM; Pricella, Wuhan, China) supplemented with 10% foetal bovine serum (FBS) (Biological Industries, Kibbutz Beit-Haemek, Israel) and 1% penicillin–streptomycin solution. The cultivation environment was maintained at 37°C, and the carbon dioxide concentration was 5%.

Reverse transcription–quantitative polymerase chain reaction

The TRIzol reagent was used to extract sample RNA from cultured cell lines (Thermo Fisher Scientific, Waltham, Massachusetts, 15596026), and an AG RNAex Pro RNA kit (Accurate Biotechnology, AG21102) was used. The protein concentration was measured using an ultramicro nucleic acid protein analyser (NanoPhotometer NP80). The genomic gDNA of the sample RNA was removed with an Evo m-mlv (Accurate Biotechnology, AG11705) kit, and then reverse transcription was performed to synthesize cDNA. Reverse transcription-polymerase chain reaction (RT-PCR) was completed with a SYBR Green Pro Taq HS premixed Kit (AG11702, accurate biotechnology). The quantitative PCR primers used were jointly designed by Beacon Designer 7.8 and Primer Premier 5.0. The cDNA was synthesized by a StepOnePlus real-time PCR system (ABI) using 2- Δ M RNA was quantified by CT and standardized to human GAPDH. The primers used for reverse transcription-quantitative polymerase chain reaction (RT–qPCR) were as follows: CXCL5 forward 5'-GCCTGTTCTAG TCCTGGTGG-3', reverse 5'-GGCATCTAAAAAGCTCA GCAATG-3'; human GAPDH forward 5'-AGAAGGCTGG GGCTCATTTG-3', and reverse 5'-AGGGGCCATCCACA GTCTTC-3'.

Western blot analysis

First, sufficient cells were collected and washed 3 times with 4°C PBS. The washed cells were fully lysed with

radio-immunoprecipitation assay (RIPA) lysis buffer (Beyotime, Shanghai, p0013b) containing 10% pmsf for 15 minutes and centrifuged at 14000 r/min for 5 minutes, after which the supernatant was extracted. We used a Bicinchoninic Acid Assay (BCA) protein assay kit to determine the protein concentration (Beyotime, P0010, Shanghai) and separated the proteins by Sodium dodecyl sulfate polyacrylamide gel electrophoresis (SDS-PAGE). Then, the proteins were transferred to polyvinylidene fluoride (PVDF) membranes (Immobilon-P, Millipore) at room temperature. Notably, 5% fat-free milk was used for blocking for 2 hours. Primary antibodies were added and incubated in a 4°C refrigerator overnight. Tris-buffered saline with 0.1% Tween-20 (TBST) was used. The blots were washed 3 times for 10 minutes each. At room temperature, secondary antibody was added, and the samples were incubated for 1 hour. TBST was used for membrane washing. The blots were washed 3 times for 10 minutes each. Finally, protein expression was detected by an enhanced chemiluminescence system.

Transfection and treatments

We transfected CXCL5 siRNA into BxPC-3 and CFPAC-1 cells. Notably, 24-well plates were used for transfection, and the cells were grown to 60%–70% confluence at the time of transfection. The cells in each well were incubated and transfected with Lipofectamine 2000 (Thermo Fisher Scientific, 11668019) diluted in serum-free medium at 37°C and 5% CO_2, and the negative control group was transfected with Lipofectamine 2000 as an empty carrier. Cells were stably transfected with Geneticin (G418; Thermo Scientific, Shanghai, China). Instantly transfected cells were harvested 48 hours later.

CCK-8 assay

We used a CCK-8 cell counting cassette to determine the changes in viability of the BxPC-3 and CFPAC-1 cell groups. In a sterile 96-well plate, the cell suspension was added to the middle wells of the plate at a density of 5000 cells/20 μL. Culture solution was added to the blank wells around the test wells to prevent experimental evaporation from affecting the results. The cells were cultured at 37°C and 5% CO2 for 48 hours and then incubated with CCK-8 reagent for 4 hours. A Multiskan microplate reader was used to measure the optical density at 480 nm (Thermo Fisher Scientific).

Cell apoptosis assay

Sufficient cells were collected, washed with PBS, and adjusted to 2×10^5/mL. Then, 200 μL of cell suspension was added to 1 mL of cold PBS at 1000 r/min and 4°C for 10 minutes. The supernatant was aspirated after centrifugation, and the process was repeated 3 times. The cell pellets were resuspended by adding 200 μL of labelling buffer. Then, 10 μL of Annexin V-FITC (Beyotime, C1062M, Shanghai) was added, mixed well in the dark, and reacted for 15 minutes at room temperature. Then, 300 μL of labelling buffer was added, and the cells were immediately detected by flow cytometry (Millipore, USA, Guava easyCyte HT).

Cell cycle analysis

The cells were resuspended in 2 mL of PBS and centrifuged at 1000 r/min for 5 minutes, after which the supernatant was removed. Then, 1 mL of PBS and 2 mL of absolute ethanol were added, and the sample was resuspended and centrifuged for 5 minutes at 1000 r/min. The fixation solution was removed, and the cells were washed twice with 2 mL of PBS. The supernatant was discarded, and 400 μL of PBS was used to resuspend the cells. Then, 50 μL of propidium iodide reagent and 50 μL of RNase (Beyotime, Shanghai; C1052) were added and incubated in a dark room for 30 minutes. Detection of the samples was performed using flow cytometry (Guava easyCyte HT).

Cell invasion assay

Transwell assays were used to analyse the invasion and migration of BxPC-3 and CFPAC-1 cells. A 24-well cell culture plate with Transwell chambers with 8 μm pores was used (Corning, USA, 354480). For cell migration experiments, the cells were washed 3 times with PBS after digestion and then made into a cell suspension with serum-free medium containing BSA, and the cell density in the cell suspension was adjusted to 5×10^5/mL. A volume of 200 μL was inoculated into the upper chamber of the Transwell chamber, and 600 μL of medium supplemented with 15% FBS was added. The cells were incubated at 37°C for 24 hours. The chamber was removed, and the culture solution in the well was discarded. PBS-washed migratory cells were fixed with 4% paraformaldehyde (Beyotime, Shanghai, P0099). The upper layer of nonmigrated cells was removed, and the cells were stained with 0.1% crystal violet for 20 minutes (Beyotime, Shanghai, C0121) and then washed 3 times with PBS. Cells in 5 randomly selected fields were observed under a microscope and photographed (Caikang Optical Instrument, Shanghai, XDS-100). For invasion experiments, 300 μL of serum-free medium at 4°C was added to 50 μL of Matrigel (Corning, USA, 356234), mixed well, and placed on ice. The Transwell chamber was then incubated for 4 hours at 37°C. The remaining experimental procedures were the same as those used for the migration experiment.

Cell colony formation assay

The cells were collected and resuspended in 10% FBS RPMI 1640 medium (11875101, Thermo Fisher Scientific). With a cell density gradient of 50, 100, or 200 cells/dish, the cells were

inoculated into a Petri dish containing 10 mL of culture medium at 37°C. The cells were incubated at 5% CO_2, 37°C, and saturated humidity for 2 weeks. The culture was terminated, the supernatant was removed, and the cells were washed twice with PBS. Notably, 5 mL of pure methanol (Beyotime, Shanghai, P0099) was added, and the cells were fixed for 15 minutes. The fixative was discarded, and the cells were stained with Giemsa staining solution for 30 minutes. The samples were washed with slow-running water, air-dried at room temperature, and counted with a microscope.

Animal experiments

Subcutaneous tumourigenesis assays were performed in nude mice. All animal surgeries were performed on the basis of the protocol authorized by the ethics committee of the Institute of Jiaxing University. For xenograft assays, NC-CXCL5 (negative control), SH-CXCL5, and OE-CXCL5 were engrafted at a density of 2×10^5/mL cells randomized, each group contained 5 mice. Four-week-old BALB/C nude mice were selected, and these cells were injected subcutaneously into the left armpit. The weights of the nude mice were measured and recorded every 3 days, and the tumour size was measured with a Vernier calliper every 3 days after tumour formation. After 23 days, the mice were exposed to CO2, and the weights of the tumours were measured.

Statistical analysis

In this experiment, *t*-tests were used to compare the data obtained from these measurements. Fisher's exact probability method, the chi-square test, and the R×C contingency table were used for qualitative data comparison. Multivariate analysis was completed by the Cox multivariate regression analysis model. The difference in survival rate between groups was determined using the log-rank method, and survival was assessed using the Kaplan-Meier method. We used the Spearman correlation analysis to investigate the correlation between CXCL5 and the infiltration levels of 3 types of T cells (CD4+, CD8+, and FOXP3). In this project, various drawing software packages were used to illustrate the results. These included Adobe Photoshop CS5, Adobe Illustrator CS6, SPSS 22.0, and GraphPad Prism 6.02. $P < .05$ indicated statistical significance.

Results

Relationships between CXCL5 levels and clinical factors

This study included 90 patients with pancreatic cancer. We collected tumour tissues and adjacent normal tissues from each patient. We further analysed the correlation between CXCL5 and clinicopathological features. We found that sex, age, tumour location, vascular invasion status, degree of differentiation, tumour TNM stage, smoking status, alcohol consumption status, and other factors were not significantly correlated with CXCL5 expression (Table 1, $P > .05$). There was no significant difference in different AJCC stages in this study, which may be limited by the sample size. It is also possible that although it is highly expressed in tumour tissue, it is not significantly correlated with the tumour AJCC stage.

Expression of CXCL5 in various pancreatic cancer cell lines and construction and verification of CXCL5-overexpressing/knockdown cell lines

We aimed to explore the differences in the expression of CXCL5 between normal tissues and various pancreatic cancer cell lines. Five pancreatic tumour cell lines were compared with the pancreatic ductal epithelial cell line HPDE6C7 (Figure 1A). Through RT-qPCR, we found that CXCL5 expression was significantly greater in BxPC-3 and CFPAC-1 cells than in the other assessed cell lines. We next aimed to further assess whether high or low expression of CXCL5 affects the migration and proliferation of tumour cells. First, we established CXCL5-overexpressing and CXCL5-knockdown cell lines using BxPC-3 and CFPAC-1 cells as the parental cell lines. Reverse transcription-polymerase chain reaction was performed to verify the CXCL5 mRNA content of BxPC-3 cells (Figure 1B) and CFPAC-1 (Figure 1D) cells, and Western blotting was performed to verify the CXCL5 protein content of BxPC-3 cells (Figure 1C) and CFPAC-1 (Figure 1E). This indicates successful cell line construction.

### Effect of CXCL5 on the proliferation and apoptosis of pancreatic cancer cells

In the CCK-8 assay, we found that the proliferation of the CXCL5-overexpressing group was obviously greater than that of the blank control group and normal group. The proliferation of cells in the CXCL5 knockdown group was relatively inhibited (Figure 2). This experiment showed that the expression of CXCL5 was directly proportional to the cell proliferation rate of these 2 tumour cell lines. To explore the effect of CXCL5 on tumour proliferation at a deeper level, cell cycle analysis was performed on BxPC-3 (Figure 3A) and CFPAC-1 (Figure 3B) cells. Most BxPC-3 cells in the CXCL5 knockdown group were in the G1 phase. In contrast, the proportion of cells in the G2/M and S phases was lower than that in the control group. In the S phase, the CXCL5 overexpression group outperformed the other groups. Similar results were observed in the CFPAC-1 cell group. Therefore, we detected cyclins by Western blotting. Knockdown of CXCL5 resulted in low cyclin E1 expression, whereas high expression of CXCL5 resulted in increased cyclin E1 expression (Figure 3C and D). But for cyclin D1, CDK4, and CDK6, this phenomenon did not occur.

Table 1. Correlation between CXCL5 and clinicopathological features of patients.

	LEVEL	CXCL5 LOW	CXCL5 HIGH	*P*
n		50	40	
Age (%)	<65	27 (54.0)	18 (45.0)	.525
	≥0.5	23 (46.0)	22 (55.0)	
Sex (%)	Male	29 (58.0)	21 (52.5)	.758
	Female	21 (42.0)	19 (47.5)	
Grade (%)	1	17 (34.0)	23 (57.5)	.051
	2	29 (58.0)	13 (32.5)	
	3	4 (8.0)	4 (10.0)	
Tumour site (%)	Head	34 (68.0)	32 (80.0)	.299
	Others	16 (32.0)	8 (20.0)	
Tumour size (%)	≤3 cm	28 (56.0)	19 (47.5)	.555
	>3cm	22 (44.0)	21 (52.5)	
Local invasion (%)	No	21 (42.0)	19 (47.5)	.758
	Yes	29 (58.0)	21 (52.5)	
Perineural invasion (%)	No	7 (14.0)	4 (10.0)	.801
	Yes	43 (86.0)	36 (90.0)	
Vascular invasion (%)	No	36 (72.0)	25 (62.5)	.465
	Yes	14 (28.0)	15 (37.5)	
Lymph node metastasis (%)	No	31 (62.0)	20 (50.0)	.354
	Yes	19 (38.0)	20 (50.0)	
T2 (%)	T1 + T2	35 (70.0)	26 (65.0)	.781
	T3 + T4	15 (30.0)	14 (35.0)	
N (%)	N0	31 (62.0)	20 (50.0)	.461
	N1	15 (30.0)	17 (42.5)	
0	N2	4 (8.0)	3 (7.5)	
M (%)	M0	48 (96.0)	37 (92.5)	.797
	M1	2 (4.0)	3 (7.5)	
AJCC stage (%)	1	21 (42.0)	14 (35.0)	.792
	2	22 (44.0)	20 (50.0)	
	3 + 4	7 (14.0)	6 (15.0)	
Smoking (%)	No	40 (80.0)	26 (65.0)	.174
	Yes	10 (20.0)	14 (35.0)	
Drinking (%)	No	41 (82.0)	32 (80.0)	1
	Yes	9 (18.0)	8 (20.0)	
Diabetes (%)	No	43 (86.0)	35 (87.5)	1
	Yes	7 (14.0)	5 (12.5)	
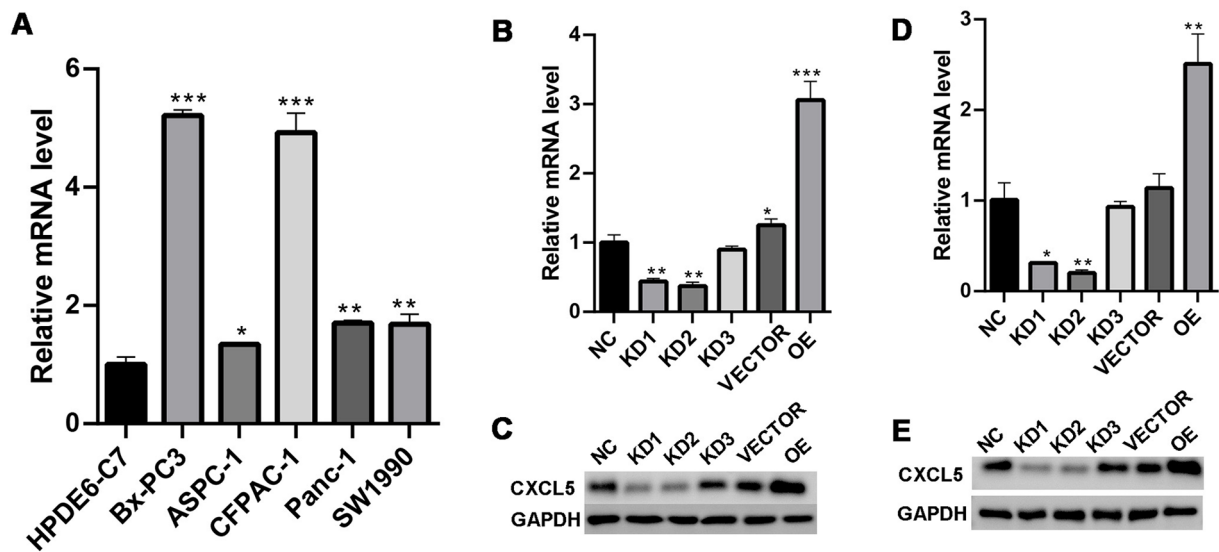
Figure 1. The expression of CXCL5 in various cells. (A) CXCL5 in various pancreatic tumour cell lines. CXCL5 expression was significantly greater in BxPC-3 cells and CFPAC-1 cells than in other cell lines. (B and C) CXCL5 expression levels in different BxPC-3 cells. (B) Detection of the CXCL5 level in control, CXCL5-overexpressing, or CXCL5-silenced cells by RT-qPCR. (C) Detection of the CXCL5 level in control, CXCL5-overexpressing, or CXCL5-silenced cells by Western blotting. (D and E) CXCL5 expression levels in different CFPAC-1 cells. (D) Detection of the CXCL5 level in control, CXCL5-overexpressing, or CXCL5-silenced cells by RT-qPCR. (E) Detection of the CXCL5 level in control, CXCL5-overexpressing, or CXCL5-silenced cells by Western blotting.
NC: negative control group; KD: knockdown group; VECTOR: blank transfection group; OE: overexpression group. $*P < .05$; $**P < .01$; $***P < .001$.
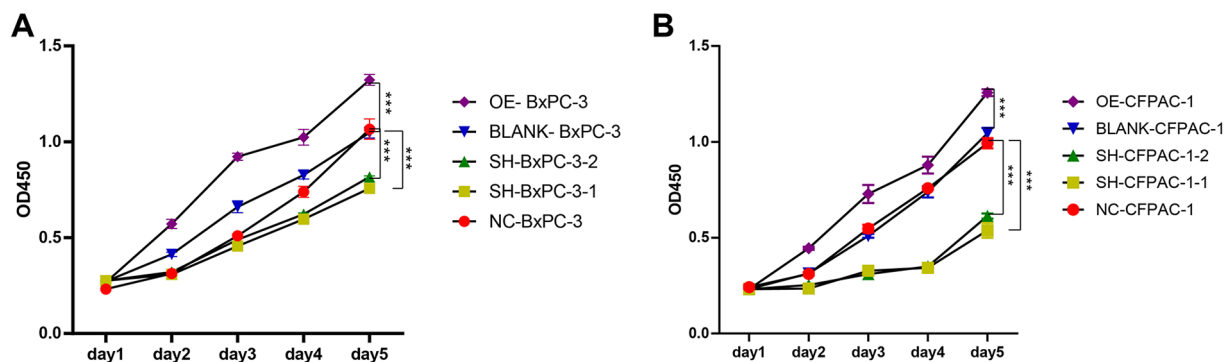
Figure 2. CCK-8 assay. The survival ability of CFPAC-1 cells and BxPC-3 cells of transfection was affected by knocking down CXCL5 and Overexpressing CXCL5. (A) CCK-8 assay of BxPC-3 cells; (B) CCK-8 assay of CFPAC-1 cells.
NC-BxPC-3: BxPC-3 negative control group.
SH-BxPC-3: BxPC-3 shRNA-mediated knockdown group.
BLANK- BxPC-3: BxPC-3 blank transfection group.
OE- BxPC-3: BxPC-3 overexpression group.
NC-CFPAC-1: CFPAC-1 negative control group.
SH-CFPAC-1: CFPAC shRNA-mediated knockdown group.
BLANK-CFPAC-1: CFPAC-1 blank transfection group.
OE-CFPAC-1: CFPAC-1 overexpression group.
$*P < .05$; $**P < .01$; $***P < .001$.

We also performed a cell colony formation assay (Figure 3G and H). In culture dishes, we found that CFPAC-1 and BxPC-3 cells with CXCL5 knockdown had obvious growth restrictions. However, the growth and proliferation of CXCL5-overexpressing CFPAC-1 and BxPC-3 cells in culture dishes were obviously enhanced. Flow cytometry was performed to detect the percentage of apoptotic cells in the 2 groups (Figure 3E and F), and we found that CXCL5 knockdown significantly enhanced cell apoptosis, while CXCL5 overexpression had the opposite effect. Through proliferation and apoptosis

assays, we found that CXCL5 overexpression is beneficial for pancreatic cancer cells.

Effects of CXCL5 on the migration and invasion of pancreatic tumour cells

Next, we explored the impact of high/low CXCL5 on invasion and migration. We performed Transwell invasion assays on CFPAC-1 and BxPC-3 cells (Figure 4A and B). SH-CXCL5 transfection and CXCL5 overexpression were compared with
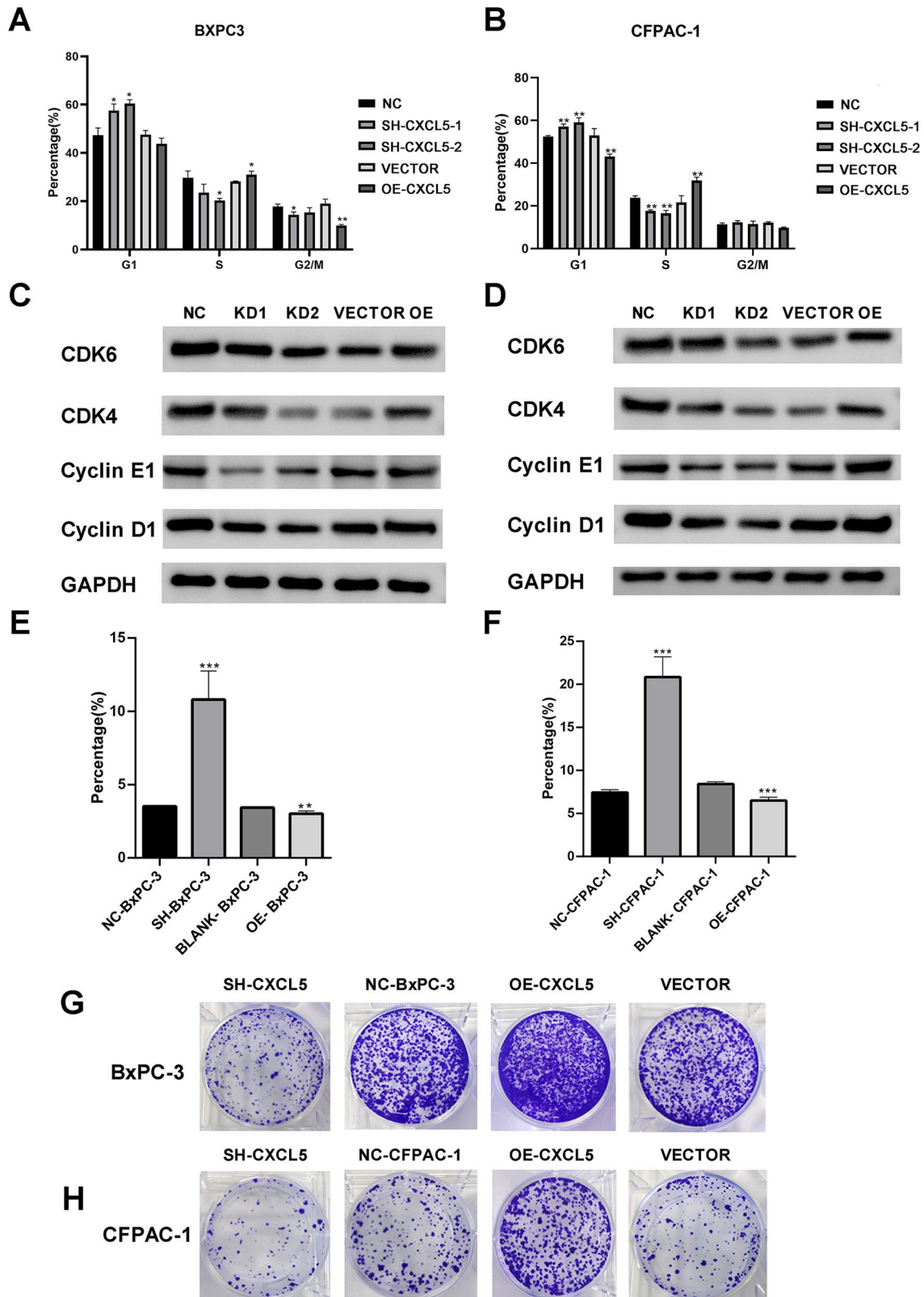
Figure 3. Effects of CXCL5 on cell cycle and clonal formation of pancreatic cancer cells. (A) Histogram of cell cycle distribution in the control, SH-CXCL5, VECTOR, and OE-CXCL5 cells of BxPC-3. (B) Histogram of cell cycle distribution in the control, SH-CXCL5, VECTOR, and OE-CXCL5 cells of CFPAC-1. (C) Cyclin was detected by Western blot in BxPC-3 cells. (D) Cyclin was detected by Western blot in CFPAC-1 cells. (E) The histogram percentage of apoptotic cells in BxPC-3. (F) The histogram percentage of apoptotic cells in CFPAC-1 cells. (G) Scanned image of plates showing different levels of colony formation. Colony formation of BxPC-3 cells. (H) Scanning image of plates showing different levels of colony formation. Colony formation of CFPAC-1 cells.
NC: negative control group; KD: knockdown group; VECTOR: blank transfection group; OE: overexpression group.
*$P < .05$; **$P < .01$; ***$P < .001$.
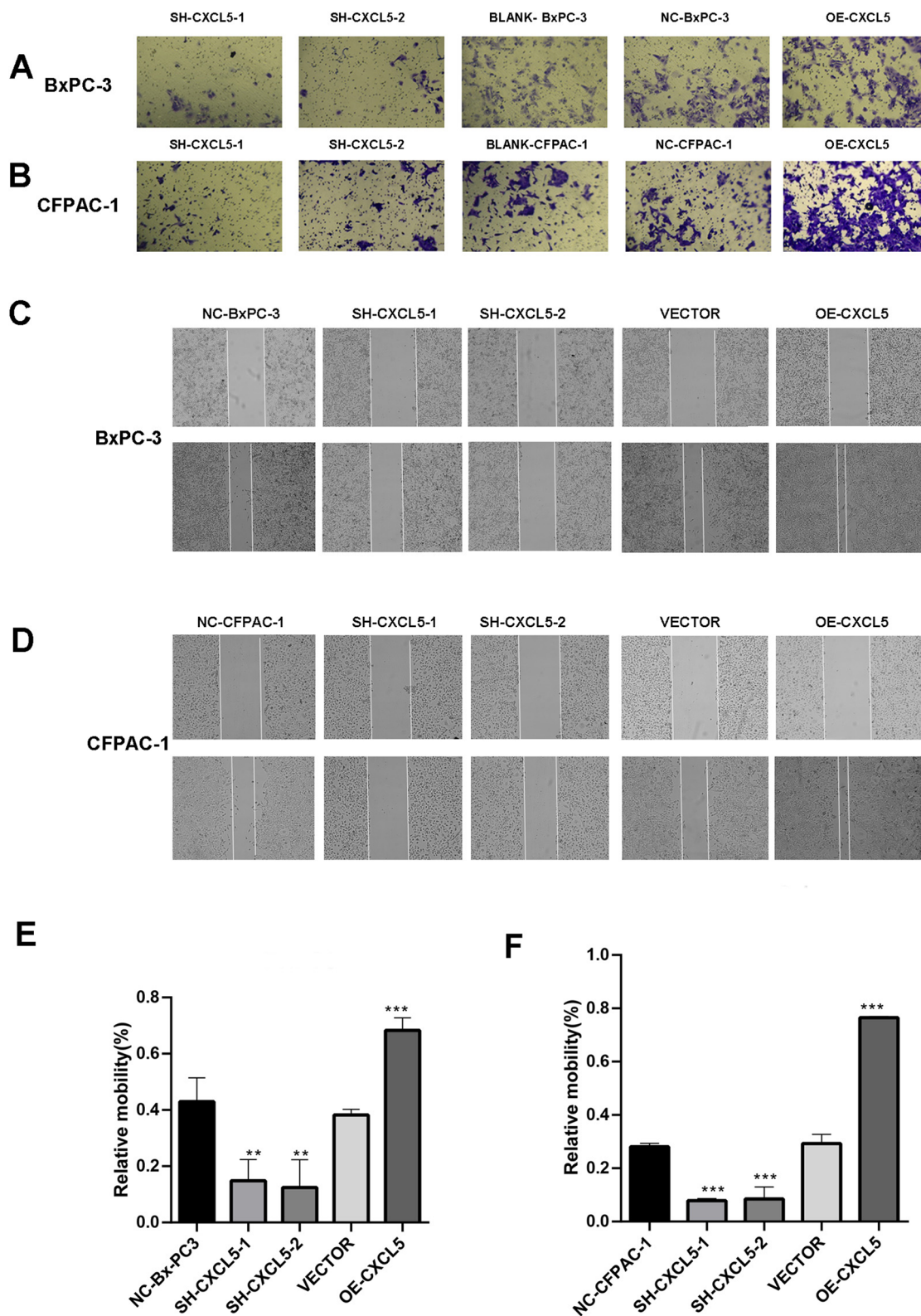
Figure 4. Effects of CXCL5 on invasion and migration of pancreatic cancer cells. (A) CXCL5 knockdown inhibits cell invasion. Transwell invasion assay: BxPC-3 cells were transfected with CXCL5 shRNA or a CXCL5 overexpression vector. (B) CXCL5 knockdown inhibited cell invasion. Transwell invasion assay: CFPAC-1 cells were transfected with CXCL5 shRNA or the CXCL5 overexpression vector. (C) The migration ability of the cells was analysed through wound healing experiments. BxPC-3 cells were transiently transfected with CXCL5 or control shRNA. (D) The migration ability of the cells was analysed through wound healing experiments. Transient transfection of CFPAC-1 cells with CXCL5 or control shRNA. (C and D) Quantification of the experimental data shown in the graphs. Magnification, 40×. The results revealed that the wound healing rate of CFPAC-1 and BxPC-3 cells could be reduced by silencing CXCL5. (E) Rates of BxPC-3 cells; (F) Rates of CFPAC-1 cells.
*$P < .05$; **$P < .01$; ***$P < .001$.
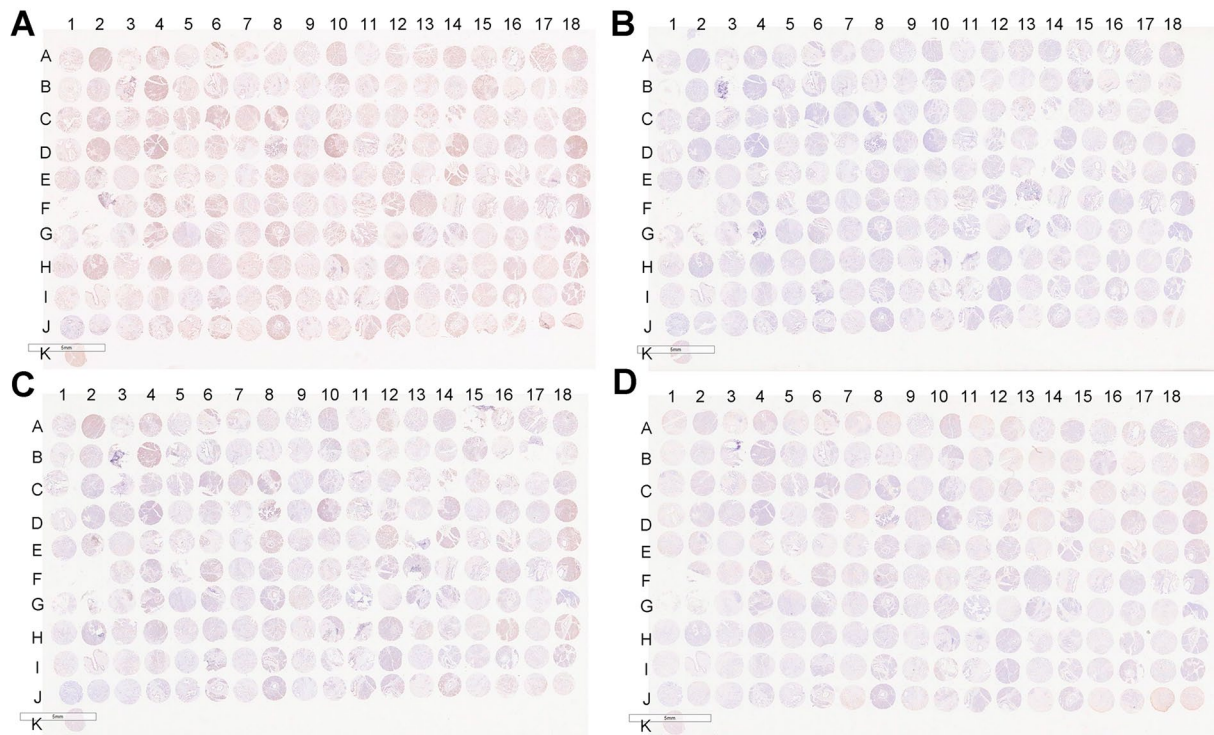
Figure 5. Expression of CXCL5, CD4, CD8, and FOXP3 in pancreatic cancer and adjacent normal tissues. (A) CXCL5 staining of adjacent tissue and corresponding tumour tissue from 90 pancreatic cancer patients. (B) CD4 staining of adjacent tissue and corresponding tumour tissue from 90 pancreatic cancer patients. (C) CD8 staining of tumour tissue and corresponding adjacent nontumour tissues from 90 pancreatic cancer patients. (D) FOXP3 staining of adjacent tissue and corresponding tumour tissue from 90 pancreatic cancer patients. The odd-numbered columns represent the intratumoural tumour tissues, and the even-numbered columns represent the paired paracancerous tissue samples.

those in the control group. The results showed that tumour cells with high expression of CXCL5 had stronger invasive ability, especially in the CFAPC-1 cell line. Therefore, whether it has the same effect on cell migration ability remains unclear. Wound healing experiments were conducted on CFPAC-1 and BxPC-3 cells. At 40× magnification (Figure 4C and D), CXCL5 silencing decreased the wound healing rate of CFPAC-1 and BxPC-3 tumour cells. By quantifying the data (Figure 4E and F), we can intuitively see that the expression of CXCL5 is directly proportional to migration ability.

Correlation analysis of CXCL5, CD4, CD8, and FOXP3 expression and immune infiltration

A total of 90 pairs of tumour tissue and adjacent tissues were used for immunohistochemistry (Figure 5), and the results were analysed. The Spearman correlation analysis indicated that there was a significant negative correlation between CXCL5 levels and the CD8 IRS ($r=-0.205$, $P=.018$; Table 2). There was no significant correlation between the CD4 IRS and CXCL5 level ($r=-0.086$, $P=.418$; Table 3). However, there was a significant positive correlation between FOXP3 IRS and CXCL5 levels ($r=0.341$, $P=.001$; Table 4). These findings suggest that the high expression of CXCL5 in pancreatic cancer may be unfavourable for cytotoxic lymphocyte infiltration. CXCL5 may be associated with the infiltration of immunosuppressive FOXP3 + T cells to form an immunosuppressive microenvironment.

Effect of CXCL5 on tumour phenotype and immune infiltration in vivo

Using nude mice, we completed a subcutaneous tumourigenesis test. Finally, we generated a negative control group, an SH-CXCL5 group, and an OE-CXCL5 group, which consisted of 3 groups of subcutaneous tumours (Figure 6A). We also calculated the tumour growth curve and average tumour weight (Figure 6B, C). The knockdown group showed slower growth and reduced tumour weight, whereas the overexpression group showed faster tumour growth and increased tumour weight.

Discussion
Chemokines are involved in immune and inflammatory responses by mediating leukocyte migration and triggering specific immune responses. There are 4 kinds of chemokines (C, CC, CXC, and CX3C) that are important targets for tumour immunotherapy.[19] At present, many chemokines are found in tumour cells. These chemokines often regulate a variety of cells and ultimately affect the occurrence and development of tumours or immune escape.[20] Studies have shown that these chemokines can induce naive T-cell infiltration in the

Table 2. CXCL5 expression level and CD8 IRS correlation.

| | | CD8 IRS | | | | | | |
		0	1	2	3	4	6	9
CXCL5	Low	0	3	7	7	5	25	3
	High	1	2	10	11	3	13	0
r							−0.250	
P							.018	

Table 3. CXCL5 expression level and CD4 IRS correlation.

| | | CD4 IRS | | | | | |
		0	1	2	3	4	6
CXCL5	Low	11	24	11	1	2	1
	High	10	22	5	0	3	0
r						−0.086	
P						.418	

Table 4. CXCL5 expression level and FOXP3 IRS correlation.

| | | FOXP3 IRS | | | | | | |
		0	1	2	3	4	6	8
CXCL5	Low	22	17	9	0	1	0	1
	High	7	13	13	2	3	1	1
r							0.341	
P							.001	

tumour microenvironment,[21] CCL1 and CCL17 can enhance the activation of CD8 + T cells,[22] CXCL9 enhances CXCR3 and monocyte tumour infiltration,[23] and CXCL12 and CXCL16 can induce tumour regression through T-cell infiltration.[24,25] The receptor axis composed of chemokines and receptors can also be involved in cellular physiological and pathological processes by inducing directional cell movement or recruiting immune effector cells.[26,27] These findings indicate that chemokines play important roles in the occurrence and development of cancer.

Pancreatic cancer is a malignant tumour with high mortality. With a unique immunosuppressive tumour microenvironment, immunotherapy against pancreatic cancer is limited.[28] Therefore, targeted immunotherapy has become a new adjuvant therapy. In this study, we found that CXCL5 not only reduced immune cell infiltration but also affected the malignant phenotype of cancer. This finding further suggested that CXCL5 may become an important target in the immunotherapy of pancreatic cancer. CXCL5 can play a role in a variety of
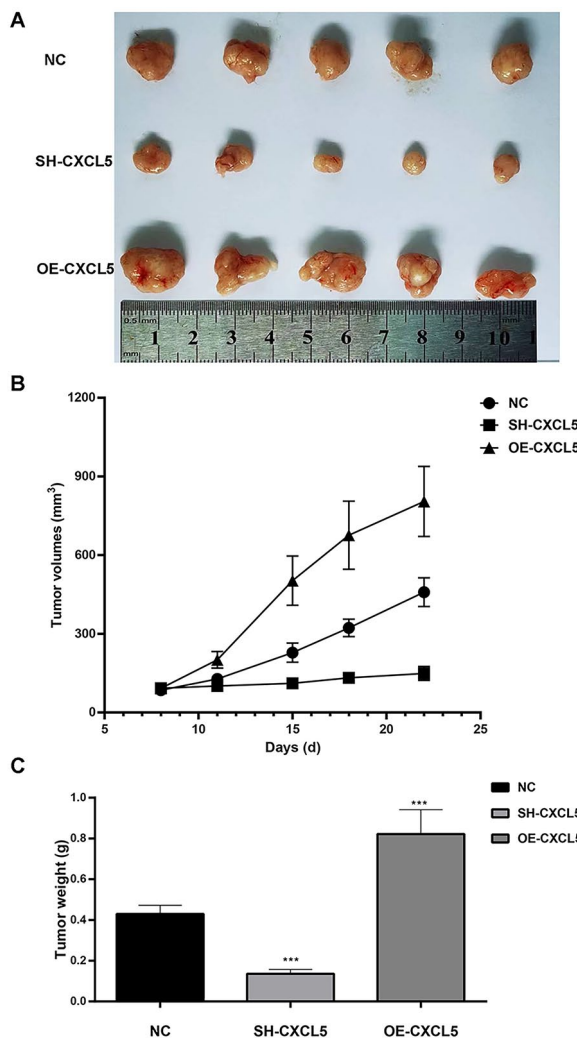
Figure 6. Knockdown of CXCL5 increased inhibition in an in vivo mouse tumour model. (A) Pictures of tumours in nude mice. (B and C). Growth curves and mean tumour weights after tumour measurements.
NC: negative control group; SH-CXCL5: CXCL5 shRNA knockdown group; OE-CXCL5: CXCL5 overexpression group.
$*P<.05; **P<.01; ***P<.001$.

cancers by inducing immune cell aggregation in the immune microenvironment.[12] It further promotes cell proliferation by changing autocrine ability while affecting the generation of derived blood vessels to promote the growth of pancreatic tumours.[29] Overexpression of CXCL5 and CXCL1 can promote immunosuppression through macrophage-derived apolipoprotein E, resulting in poor survival in patients.[30] Tumour invasion and metastasis are among the determinants of patient prognosis. The high expression of CXCL5 in PDAC can be activated by receptor tyrosine kinase discoid domain receptor 1 and then the formation of neurotrophic extracellular traps,[31] which promote tumour growth and metastasis. Gamma aminobutyric acid, a receptor pi subunit, induces Ca^{2+} and activated nuclear factor κB signalling, which in turn leads to the overexpression of CXCL5 and CCL20. This process promotes

macrophage infiltration and ultimately contributes to tumour metastasis.[32] In addition, studies have shown that knockdown of CXCL5 can reduce resistance to gemcitabine in the treatment of pancreatic cancer.[33] Knockdown of CXCL5 expression in the treatment of bladder cancer can affect the NF-κB pathway to effectively attenuate resistance to mitomycin C.[34] In sunitinib-resistant cells, researchers also found that CXCL5 was significantly upregulated.[35] CXCL5 not only has excellent research value in improving drug resistance but also improves the therapeutic efficacy of the tyrosine kinase inhibitor gefitinib without increasing side effects in the combined treatment of lung cancer.[36] Therefore, targeted inhibitors against CXCL5 could become a new way to attenuate drug resistance and could be used as adjuvant drugs.

The metastasis of malignant tumours is also positively correlated with the expression of CXCL5. In the tumour microenvironment, CXCL5 can affect the local metastasis of advanced melanoma, which is mainly related to neutrophil infiltration.[37] High CXCL5 in colorectal cancer liver metastasis and gastric cancer lymphatic metastasis predicts high metastasis risk.[38,39] The expression of CXCL5 is greater in highly metastatic hepatocellular carcinoma than in other types.[40] CXCL5 expression in patients with metastatic prostate cancer was greater than that in patients with primary prostate cancer.[41] Therefore, CXCL5 shows strong potential as a targeted cytokine in immunotherapy.

CXCL5 in pancreatic cancer can promote migration and invasion through the cxcl5/cxcr2 axis. The Cxcl5/cxcr2 axis plays a bridging role in the microenvironment of solid tumours. It is involved in recruiting immune cells and promoting tumour growth and proliferation.[42] The cxcl5/cxcr2 axis affects the growth of breast cancer,[43] nasopharyngeal carcinoma,[44] thyroid cancer,[45] and other tumours. In the potential mechanism by which CXCL5 acts on pancreatic cancer cells, some scholars have found that there is a positive correlation between epithelial-mesenchymal transition (EMT) markers (SNAI2 and TWIST1) and CXCL5 in pancreatic cancer.[46] In colon cancer, a team of experts reported that high expression of CXCL5 induced EMT in a CXCR2-dependent manner. This process mainly depends on the ERK/Elk-1/Snail and AKT/GSK3β/β-catenin pathways.[47] The CXCR2/CXCL5 axis, which activates the PI3K/Akt/GSK-3β/Snail signalling pathway, further induces EMT and is involved in the progression of hepatocellular carcinoma.[48] Therefore, the CXCR2/CXCL5 axis can induce EMT, which may be a potential mechanism by which CXCL5 is involved in the occurrence and development of pancreatic cancer.

To explore the relationships between the malignant phenotype and immune infiltration of pancreatic cancer patients and the expression of CXCL5, we first explored the associations between CXCL5 expression and clinical pathophysiological characteristics. Unfortunately, the correlations were not significant. We further selected cells with high CXCL5 levels and constructed and verified CFPAC-1 and BxPC-3 cells with CXCL5 overexpression or knockdown. We used the 2 constructed cell lines and control cells for the CCK-8 assay, cell proliferation and apoptosis assay, cell invasion and migration assay, and so on. Our study found that the expression level of CXCL5 in tumour cell proliferation can affect cell proliferation, and this effect is often proportional to the expression of CXCL5. Further experiments showed that most cells in the knockdown CXCL5 group exhibited cell cycle arrest in the G1 phase, which may be due to the impact of knockdown CXCL5 on the low expression of cyclin E1. Our experiment of detecting cyclin by Western blot confirmed this point. At the same time, flow cytometry also found that CXCL5 knockdown significantly enhanced cell apoptosis. Overall, we found that CXCL5 overexpression was beneficial to pancreatic cancer cells. Studies have revealed that high expression of CXCL5 enhances the malignant phenotype of pancreatic tumour cells. The level of expression of CXCL5 and the infiltration of CD8, CD4, and FOXP3T cells were explored by immunohistochemistry. The CXCL5 expression level was related to the CD8 IRS. To verify this result, we generated subcutaneous tumour models in nude mice after obtaining Ethics Committee approval from the Institute of Jiaxing Second Hospital. Mouse experiments showed that the average weight of tumour in the knockdown group was reduced, and the growth curve analysis also found that the tumour in the knockdown group grew slowly. This further illustrates high CXCL5 promoted the growth of subcutaneous tumours in mice.

Of course, there are still limitations in our study. First of all, the specific pathway through which CXCL5 can promote tumour progression needs to be further studied. In addition, we observed that the expression of CXCL5 was correlated with CD8 and FOXP3, but we did not deeply explore the liquid and liquid mechanism of CXCL5 affecting tumour immunity.

Conclusions

In this study, we aimed to explore the relationships between CXCL5 and malignant phenotypes and immune infiltration. We analysed the associations between the clinicopathological characteristics of pancreatic cancer patients and CXCL5 levels. Cell lines with high expression of CXCL5 were screened and validated through sufficient experiments. We found that CXCL5 can promote a malignant phenotype, and high expression of CXCL5 often indicates poor patient prognosis. Therefore, CXCL5 may become a valuable new target for future immunotherapy. However, accurate treatment of cancer has gradually become an important point of clinical treatment. This study failed to fully explore the possible regulatory mechanism and signal pathway of CXCL5 on pancreatic cancer. So, the underlying molecular mechanism of CXCL5 regulation still needs to be further explored. Whether CXCL5 can play an effective role in clinical immunotherapy in the future remains to be further verified.

Author Contributions

YYS and BW contributed to the concept and design of the research. JS and XGW reviewed and approved the study design.

TW contributed to writing – original draft and cytological experiment. SJL contributed to data curation and cytological experiment. MYZ contributed to animal experiments on mice. XGW contributed to writing, review, and editing. TW contributed to clinical sample collection. All authors contributed to the drafting of the article.

Availability of Data and Materials

The data presented in this study are available upon request from the corresponding author.

Consent for Publication

All patients signed informed consent to receive clinical samples and clinical information. All patients agreed to publication.

Ethics Approval and Consent to Participate

This research was approved by the Ethical Committee of the Second Affiliated Hospital of Jiaxing University, Jiaxing, China (Ethics Approval No. JXEY-2020SW064, Date: 29 July 2019). The animal study was approved by the Ethical Committee of Jiaxing University, Jiaxing, China (Ethics Approval No. JUMC2019-061, Date: April 30, 2019). All patients agreed to participate in the study and signed the informed consent form.

ORCID iD

Tao Wang [ID] https://orcid.org/0009-0005-5741-0267

REFERENCES

1. Siegel RL, Miller KD, Wagle NS, Jemal A. Cancer statistics, 2023. *CA Cancer J Clin*. 2023;73:17-48. doi:10.3322/caac.21763

2. Fesinmeyer MD, Austin MA, Li CI, De Roos AJ, Bowen DJ. Differences in survival by histologic type of pancreatic cancer. *Cancer Epidemiol Biomarkers Prev*. 2005;14:1766-1773. doi:10.1158/1055-9965.EPI-05-0120

3. Wood LD, Canto MI, Jaffee EM, Simeone DM. Pancreatic cancer: pathogenesis, screening, diagnosis, and treatment. *Gastroenterology*. 2022;163:386-402. doi:10.1053/j.gastro.2022.03.056

4. Aroldi F, Bertocchi P, Rosso E, Prochilo T, Zaniboni A. Pancreatic cancer: promises and failures of target therapies. *Rev Recent Clin Trials*. 2016;11:33-38. doi:10.2174/1574887110666150930122720

5. Mukherji R, Debnath D, Hartley ML, Noel MS. The role of immunotherapy in pancreatic cancer. *Curr Oncol*. 2022;29:6864-6892. doi:10.3390/curroncol29100541

6. Herting CJ, Karpovsky I, Lesinski GB. The tumor microenvironment in pancreatic ductal adenocarcinoma: current perspectives and future directions. *Cancer Metastasis Rev*. 2021;40:675-689. doi:10.1007/s10555-021-09988-w

7. Zhou W, Zhou Y, Chen X, et al. Pancreatic cancer-targeting exosomes for enhancing immunotherapy and reprogramming tumor microenvironment. *Biomaterials*. 2021;268:120546. doi:10.1016/j.biomaterials.2020.120546

8. Sherman MH, Beatty GL. Tumor microenvironment in pancreatic cancer pathogenesis and therapeutic resistance. *Annu Rev Pathol*. 2023;18:123-148. doi:10.1146/annurev-pathmechdis-031621-024600

9. Cortesi M, Zanoni M, Pirini F, et al. Pancreatic cancer and cellular senescence: tumor microenvironment under the spotlight. *Int J Mol Sci*. 2021;23:254. doi:10.3390/ijms23010254

10. Tang Y, Xu X, Guo S, et al. An increased abundance of tumor-infiltrating regulatory T cells is correlated with the progression and prognosis of pancreatic ductal adenocarcinoma. *PLoS ONE*. 2014;9:e91551. doi:10.1371/journal.pone.0091551

11. Bai M, Zheng Y, Liu H, Su B, Zhan Y, He H. CXCR5+ CD8+ T cells potently infiltrate pancreatic tumors and present high functionality. *Exp Cell Res*. 2017;361:39-45. doi:10.1016/j.yexcr.2017.09.039

12. Zhang R, Liu Q, Peng J, et al. CXCL5 overexpression predicts a poor prognosis in pancreatic ductal adenocarcinoma and is correlated with immune cell infiltration. *J Cancer*. 2020;11:2371-2381. doi:10.7150/jca.40517

13. Ando Y, Ohuchida K, Otsubo Y, et al. Necroptosis in pancreatic cancer promotes cancer cell migration and invasion by release of CXCL5. *PLoS ONE*. 2020;15:e0228015. doi:10.1371/journal.pone.0228015

14. Steele CW, Karim SA, Leach JDG, et al. CXCR2 inhibition profoundly suppresses metastases and augments immunotherapy in pancreatic ductal adenocarcinoma. *Cancer Cell*. 2016;29:832-845. doi:10.1016/j.ccell.2016.04.014

15. Qi Y, Zhao W, Li M, et al. High C-X-C motif chemokine 5 expression is associated with malignant phenotypes of prostate cancer cells via autocrine and paracrine pathways. *Int J Oncol*. 2018;53:358-370. doi:10.3892/ijo.2018.4388

16. Dang H, Wu W, Wang B, et al. CXCL5 plays a promoting role in osteosarcoma cell migration and invasion in autocrine- and paracrine-dependent manners. *Oncol Res*. 2017;25:177-186. doi:10.3727/096504016X14732772150343

17. Yang Y, Hou J, Shao M, et al. CXCL5 as an autocrine or paracrine cytokine is associated with proliferation and migration of hepatoblastoma HepG2 cells. *Oncol Lett*. 2017;14:7977-7985. doi:10.3892/ol.2017.7236

18. Hu B, Fan H, Lv X, Chen S, Shao Z. Prognostic significance of CXCL5 expression in cancer patients: a meta-analysis. *Cancer Cell Int*. 2018;18:68. doi:10.1186/s12935-018-0562-7

19. Dubinett SM, Lee JM, Sharma S, Mulé JJ. Chemokines: can effector cells be redirected to the site of the tumor. *Cancer J*. 2010;16:325-335. doi:10.1097/PPO.0b013e3181eb33bc

20. Nagarsheth N, Wicha MS, Zou W. Chemokines in the cancer microenvironment and their relevance in cancer immunotherapy. *Nat Rev Immunol*. 2017;17:559-572. doi:10.1038/nri.2017.49

21. Yu P, Lee Y, Liu W, et al. Priming of naive T cells inside tumors leads to eradication of established tumors. *Nat Immunol*. 2004;5:141-149. doi:10.1038/ni1029

22. Henry CJ, Ornelles DA, Mitchell LM, Brzoza-Lewis KL, Hiltbold EM. IL-12 produced by dendritic cells augments CD8+ T cell activation through the production of the chemokines CCL1 and CCL17. *J Immunol*. 2008;181:8576-8584. doi:10.4049/jimmunol.181.12.8576

23. Pan J, Burdick MD, Belperio JA, et al. CXCR3/CXCR3 ligand biological axis impairs RENCA tumor growth by a mechanism of immunoangiostasis. *J Immunol*. 2006;176:1456-1464. doi:10.4049/jimmunol.176.3.1456

24. Matsumura S, Wang B, Kawashima N, et al. Radiation-induced CXCL16 release by breast cancer cells attracts effector T cells. *J Immunol*. 2008;181:3099-3107. doi:10.4049/jimmunol.181.5.3099

25. Zhang T, Somasundaram R, Berencsi K, et al. CXC chemokine ligand 12 (stromal cell-derived factor 1 alpha) and CXCR4-dependent migration of CTLs toward melanoma cells in organotypic culture. *J Immunol*. 2005;174:5856-5863. doi:10.4049/jimmunol.174.9.5856

26. Zlotnik A, Yoshie O. The chemokine superfamily revisited. *Immunity*. 2012;36:705-716. doi:10.1016/j.immuni.2012.05.008

27. Luster AD. Chemokines—chemotactic cytokines that mediate inflammation. *N Engl J Med*. 1998;338:436-445. doi:10.1056/NEJM199802123380706

28. Banerjee K, Kumar S, Ross KA, et al. Emerging trends in the immunotherapy of pancreatic cancer. *Cancer Lett*. 2018;417:35-46. doi:10.1016/j.canlet.2017.12.012

29. Li A, King J, Moro A, et al. Overexpression of CXCL5 is associated with poor survival in patients with pancreatic cancer. *Am J Pathol*. 2011;178:1340-1349. doi:10.1016/j.ajpath.2010.11.058

30. Kemp SB, Carpenter ES, Steele NG, et al. Apolipoprotein E promotes immune suppression in pancreatic cancer through NF-κB-mediated production of CXCL1. *Cancer Res*. 2021;81:4305-4318. doi:10.1158/0008-5472.CAN-20-3929

31. Deng J, Kang Y, Cheng CC, et al. DDR1-induced neutrophil extracellular traps drive pancreatic cancer metastasis. *JCI Insight*. 2021;6:e146133. doi:10.1172/jci.insight.146133

32. Jiang SH, Zhu LL, Zhang M, et al. GABRP regulates chemokine signalling, macrophage recruitment and tumour progression in pancreatic cancer through tuning KCNN4-mediated Ca2+ signalling in a GABA-independent manner. *Gut*. 2019;68:1994-2006. doi:10.1136/gutjnl-2018-317479

33. Lee NH, Ma Y, Ang CS, et al. CXCL5 knockdown attenuated gemcitabine resistance of pancreatic cancer through regulation of cancer cells and tumour stroma. *Am J Transl Res*. 2023;15:2676-2689

34. Wang C, Li A, Yang S, Qiao R, Zhu X, Zhang J. CXCL5 promotes mitomycin C resistance in non-muscle invasive bladder cancer by activating EMT and NF-κB pathway. *Biochem Biophys Res Commun*. 2018;498:862-868. doi:10.1016/j.bbrc.2018.03.071

35. Giuliano S, Dufies M, Ndiaye PD, et al. Resistance to lysosomotropic drugs used to treat kidney and breast cancers involves autophagy and inflammation and converges in inducing CXCL5. *Theranostics*. 2019;9:1181-1199. doi:10.7150/thno.29093

36. Kuo PL, Huang MS, Hung JY, et al. Synergistic effect of lung tumor-associated dendritic cell-derived HB-EGF and CXCL5 on cancer progression. *Int J Cancer*. 2014;135:96-108. doi:10.1002/ijc.28673

37. Soler-Cardona A, Forsthuber A, Lipp K, et al. CXCL5 facilitates melanoma cell-neutrophil interaction and lymph node metastasis. *J Invest Dermatol*. 2018;138:1627-1635. doi:10.1016/j.jid.2018.01.035

38. Cui D, Zhao Y, Xu J. Activated CXCL5-CXCR2 axis promotes the migration, invasion and EMT of papillary thyroid carcinoma cells via modulation of β-catenin pathway. *Biochimie*. 2018;148:1-11. doi:10.1016/j.biochi.2018.02.009

39. Miyazaki H, Patel V, Wang H, Edmunds RK, Gutkind JS, Yeudall WA. Down-regulation of CXCL5 inhibits squamous carcinogenesis. *Cancer Res*. 2006;66:4279-4284. doi:10.1158/0008-5472.CAN-05-4398

40. Xu XJ, Yang BW, Gong FX, et al. [Expression and role of CXC chemokine 5 in liver cancer cells]. *Zhonghua Yi Xue Za Zhi*. 2012;92:2716-2719.

41. Roca H, Jones JD, Purica MC, et al. Apoptosis-induced CXCL5 accelerates inflammation and growth of prostate tumor metastases in bone. *J Clin Invest*. 2018;128:248-266. doi:10.1172/JCI92466

42. Zhang W, Wang H, Sun M, et al. CXCL5/CXCR2 axis in tumor microenvironment as potential diagnostic biomarker and therapeutic target. *Cancer Commun (Lond)*. 2020;40:69-80. doi:10.1002/cac2.12010

43. Romero-Moreno R, Curtis KJ, Coughlin TR, et al. The CXCL5/CXCR2 axis is sufficient to promote breast cancer colonization during bone metastasis. *Nat Commun*. 2019;10:4404. doi:10.1038/s41467-019-12108-6

44. Qiu WZ, Zhang HB, Xia WX, et al. The CXCL5/CXCR2 axis contributes to the epithelial-mesenchymal transition of nasopharyngeal carcinoma cells by activating ERK/GSK-3β/snail signalling. *J Exp Clin Cancer Res*. 2018;37:85. doi:10.1186/s13046-018-0722-6

45. Cui D, Zhao Y, Xu J. Activation of CXCL5-CXCR2 axis promotes proliferation and accelerates G1 to S phase transition of papillary thyroid carcinoma cells and activates JNK and p38 pathways. *Cancer Biol Ther*. 2019;20:608-616. doi:10.1080/15384047.2018.1539289

46. Wang ZZ, Li XT, Li Q J, Zhou JX. Targeting CXCL5 in pancreatic cancer cells inhibits cancer xenograft growth by reducing proliferation and inhibiting EMT progression. *Dig Dis Sci*. 2023;68:841-851. doi:10.1007/s10620-022-07529-1

47. Zhao J, Ou B, Han D, et al. Tumor-derived CXCL5 promotes human colorectal cancer metastasis through activation of the ERK/Elk-1/Snail and AKT/GSK3β/β-catenin pathways. *Mol Cancer*. 2017;16:70. doi:10.1186/s12943-017-0629-4

48. Zhou SL, Zhou ZJ, Hu ZQ, et al. CXCR2/CXCL5 axis contributes to epithelial-mesenchymal transition of HCC cells through activating PI3K/Akt/GSK-3β/Snail signaling. *Cancer Lett*. 2015;358:124-135. doi:10.1016/j.canlet.2014.11.044